Description of initial numerical codes and conceptual model (undisturbed and disturbed host rocks)

FORGE Report D4.5/D5.5 – VER.0

	Name	Organisation	Signature	Date
Compiled	Pierre Gerard	University of Liege		February 2010
Verified				
Approved	RP Shaw	BGS		25th March 2010

Keywords

.

Bibliographical reference

P Gerard. 2010. Description of initial numerical codes and conceptual model (undisturbed and disturbed host rocks).

FORGE Report D4.5/D5.5. 22pp.

Euratom 7th Framework Programme Project: FORGE

Fate of repository gases (FORGE)

The multiple barrier concept is the cornerstone of all proposed schemes for underground disposal of radioactive wastes. The concept invokes a series of barriers, both engineered and natural, between the waste and the surface. Achieving this concept is the primary objective of all disposal programmes, from site appraisal and characterisation to repository design and construction. However, the performance of the repository as a whole (waste, buffer, engineering disturbed zone, host rock), and in particular its gas transport properties, are still poorly understood. Issues still to be adequately examined that relate to understanding basic processes include: dilational versus visco-capillary flow mechanisms; long-term integrity of seals, in particular gas flow along contacts; role of the EDZ as a conduit for preferential flow; laboratory to field up-scaling. Understanding gas generation and migration is thus vital in the quantitative assessment of repositories and is the focus of the research in this integrated, multi-disciplinary project. The FORGE project is a pan-European project with links to international radioactive waste management organisations, regulators and academia, specifically designed to tackle the key research issues associated with the generation and movement of repository gasses. Of particular importance are the long-term performance of bentonite buffers, plastic clays, indurated mudrocks and crystalline formations. Further experimental data are required to reduce uncertainty relating to the quantitative treatment of gas in performance assessment. FORGE will address these issues through a series of laboratory and field-scale experiments, including the development of new methods for up-scaling allowing the optimisation of concepts through detailed scenario analysis. The FORGE partners are committed to training and CPD through a broad portfolio of training opportunities and initiatives which form a significant part of the project.

Further details on the FORGE project and its outcomes can be accessed at www.FORGEproject.org.

Contact details:

Pierre Gerard, Robert Charlier, Frédéric Collin
University of Liege

Roméo Fernandes, Sylvie Granet
EDF

Diego Arnedo, Sebastià Olivella
Universitat Politècnica de Barcelona

Description of initial numerical codes and conceptual model (undisturbed and disturbed host rocks)

Forge Project – Deliverables 4.5 and 5.5

Pierre Gerard, Robert Charlier, Frédéric Collin
Université de Liège

Roméo Fernandes, Sylvie Granet
EDF

Diego Arnedo, Sebastià Olivella
Universitat Politècnica de Barcelona

February 2010

Content

1. Introduction

In the framework of the Forge project, numerical simulations of laboratory and in-situ tests highlighting the gas migration processes in the repository will be performed by different teams (Université de Liège - ULg, Electricité de France – EDF and Universitat Politècnica de Catalunya – UPC). This report describes the initial state of the numerical codes and the main conceptual models used by each team at the beginning of the project.

The different finite element codes are Lagamine (ULg), Aster (EDF) and Code_Bright (UPC). All these codes deal with thermo-hydro-mechanical problems with partial saturation in porous media, including the gas transfers. However, the thermal problem will not be considered in the analysis to be performed within WP4 and WP5.

The types of analyses can be 1D (uniaxial confined strain or axisymetrical), 2D (plane strain, plane stress and axisymetrical) and fully 3D. The types of boundary conditions are:

- forces and displacement rate in any spatial direction for the mechanical problems;
- mass flow rate of water and air prescribed and liquid/gas pressure prescribed for the hydraulic problems;
- heat flow rate prescribed and temperature prescribed for the thermal problems.

Hereafter are presented the general framework for unsaturated porous media. The main conceptual models used by each team for the modelling of the gas migration are emphasized.

2. General framework for unsaturated porous media

The balance equations for unsaturated porous media are firstly recalled. Then the constitutive equations of the mechanical and the fluid transfers problems are described, with special emphasis on the different coupling existing between the mechanical and the hydraulic parts. The different models used by each team for the modelling of the gas migration in host rocks are presented. The equilibrium restrictions are finally described.

The general framework for the modelling of unsaturated porous media is detailed for a binary fluid mixture composed by water and air. The balance equations and the constitutive relations can be easily extended for other binary fluid mixtures of water and other gas species (hydrogen, nitrogen, helium, argon…). In these cases, the presence of air in the porous media is neglected and some gas parameters have to be modified (see section 2.5).

2.1. Balance equations of a porous medium

In the numerical study, the geomaterials of the geological layer are porous media generally considered as the superposition of several continua (Coussy, 1995): the solid skeleton (grains assembly) and the fluid phases (water, air, oil...). Based on averaging theories (Hassanizadeh and Gray, 1979a, 1979b), Lewis and Schrefler (2000) proposed the governing equations for the full dynamic behaviour of a partially saturated porous medium composed of three species (mineral, water and air) distributed in three phases (solid, liquid and gaseous phases). It is

assumed that the mineral species and the solid phase coincide. However, the liquid phase may contain dissolved air and the gas phase is a mixture of dry air and water vapour.

Hereafter the balance equations are restricted for quasi-static problem with isothermal conditions. The unknowns of the mechanical and the flow problems are respectively the displacements u_i, the water pressure p_w and the gas pressure p_g. In the following developments, the balance equations are written in the current solid configuration (updated Lagrangian formulation).

2.1.1. Balance of momentum

In the mixture balance of momentum equation, the interaction forces between fluid phases and grain skeleton cancels. This equation reads:

$$div\left(\underline{\underline{\sigma}}\right)+\left(\rho_s(1-\phi)+S_{r,w}\rho_w\phi+\left(1-S_{r,w}\right)\rho_g\phi\right)\underline{g}=0 \qquad (1)$$

where ϕ is the porosity, ρ_s is the solid grain density, ρ_w is the water density, ρ_g is the gas density, $S_{r,w}$ is the water relative saturation, $\underline{\underline{\sigma}}$ is the total (Cauchy) stress tensor and $\underline{g}$ is the gravity acceleration.

2.1.2. Solid mass balance equations

The balance equations are expressed in the moving current configuration through a Lagrangian actualised formulation. According to these assumptions, the mass balance equation of the solid skeleton is necessary met. For a given mixture volume V, the mass balance equation reads:

$$\frac{\partial\rho_s\left(1-\phi\right)\Omega}{\partial t}=0 \qquad (2)$$

where t is the time and Ω is the volume of the porous medium.

2.1.3. Fluid mass balance equations

Following the ideas of Panday (1957) and Olivella (1994), the fluid mass balance equations are written for each chemical species (i.e. water and air). In this way the terms related to the phase transfer cancel. The mass conservation equations for the water and gas species have the same form whatever the gas component (air, hydrogen, nitrogen…). Hereafter the mass conservation equations for the water and gas species are respectively presented, in the particular case of a gaseous mixture of water vapour and dry air:

$$\underbrace{div\left(\rho_w\underline{q}_l\right)+\frac{\partial}{\partial t}\left(\rho_w\phi S_{r,w}\right)-Q_w}_{\text{Liquid water}}+\underbrace{div\left(\underline{i}_v+\rho_v\underline{q}_g\right)+\frac{\partial}{\partial t}\left(\rho_v\phi\left(1-S_{r,w}\right)\right)-Q_v}_{\text{Water vapour}}=0 \qquad (3)$$

$$\underbrace{div\left(\rho_a \underline{q}_g + \underline{i}_a\right) + \frac{\partial}{\partial t}\left(\rho_a \phi\left(1 - S_{r,w}\right)\right) - Q_a}_{\text{Dry air in gaseous phase}} + \underbrace{div\left(\rho_{a-d} \underline{q}_l + \underline{i}_{a-d}\right) + \frac{\partial}{\partial t}\left(\rho_{a-d} \phi S_{r,w}\right) - Q_{a-d}}_{\text{Dissolved air in water}} = 0 \quad (4)$$

where ρ_a is the density of air; $\underline{q}_l$ and $\underline{q}_g$ are the advective flux of liquid and gaseous phases, respectively; $\underline{i}_v$ (=-$\underline{i}_a$) and $\underline{i}_{a\text{-}d}$ are the non-advective flux of water vapour and dry air; Q_w, Q_v, Q_a and $Q_{a\text{-}d}$ are the sink terms of the different species.

2.2. Constitutive equations

The constitutive equations are key components of the formulation. They describe the specific behaviour of the porous medium. Moreover the coupling phenomena are often reflected in the constitutive equations.

2.2.1. Stress-strain behaviour

In order to reproduce the stress-strain behaviour of partially saturated porous media, as the shear strength or the collapse phenomena, two separates stress variables are needed. Two main approaches exist. The first one uses the Bishop's effective stress and the suction s $\left(= p_g - p_w\right)$. The Bishop's effective stress is expressed by (Nuth & Laloui, 2008):

$$\sigma' = \sigma - b\left(S_{rw} p_w + \left(1 - S_{rw}\right) p_g\right) \quad (5)$$

where σ' is the Bishop's effective stress, σ is the total stress and b is the Biot coefficient.

Other approaches use two separate stress variables, typically net stresses σ^* and suction s $\left(= p_g - p_w\right)$. Net stress is defined as the excess of total stress over gas pressure:

$$\sigma^* = \sigma - p_g \quad (6)$$

The general form of the unsaturated constitutive models can be expressed as:

$$d\underline{\underline{\sigma}}'^{/*} = \underline{\underline{D}} d\underline{\varepsilon} + \underline{\underline{h}} d\underline{s} \quad (7)$$

with $\underline{\underline{\sigma}}'^{/*}$ the Bishop's effective stress or the net stress, $\underline{\varepsilon}$ the strain tensor, $\underline{\underline{D}}$ and $\underline{\underline{h}}$ the constitutive matrix, respectively for the strain an the suction tensors.

Owing the high preconsolidation pressure of argillite, the plastic behaviour of argillaceous rocks is mainly controlled by the shear strength, and not by the collapse phenomena. Using only the Bishop's effective stress allows thus the reproduction of the behaviour, which is the option frequently used in the modelling of host rocks behaviour.

Different constitutive models are implemented in the finite element codes:

- elastic model;
- elastoplastic model perfectly plastic, with different yield surface (Mohr-Coulomb, van Eekelen, Drucker-Prager) and potential dilatancy, hardening/softening;
- Cam-Clay model;
- Hoek & Brown model;
- Barcelona Basic Mode (Alonso et al.,1990), which allows the description of the volumetric collapse (compression) behaviour upon wetting;
- damage model;
- damage – elastoplastic model (Code Bright), which considers the argillaceous rock as a composite material made of a clay matrix interlocked by bond. Clay matrix behaviour is modelled through an elastoplastic constitutive law, typical of soils. Bonds are modelled through a damage elastic law (Carol et al., 2001), typical of quasi-brittle materials. A coupling parameter gives the relative importance of clay and bond response for the composite material. This law applies to material having a response transitional between that of a soil and a rock. The mathematical formulation of the damage – elastoplastic model is detailed in the appendix;
- viscoplastic model using a Drucker Prager criterion (EDF), the formulation of this model is detailed in the appendix.

2.2.2. Solid density variation

For the considered materials and stress levels around radioactive waste disposals, the solid grain deformability is no more negligible and the general Biot framework (Biot, 1941) is used to model the hydromechanical coupled terms. Following the ideas of Biot, Coussy (2004) proposed a thermodynamical framework of the problem, which leads to the expression of the porosity variation:

$$\dot{\phi} = (b-\phi)\left[\frac{S_{r,w}}{k_s}\,\dot{p}_w + \frac{1-S_{r,w}}{k_s}\,\dot{p}_g + \frac{\dot{\Omega}}{\Omega}\right] \tag{8}$$

where b is the Biot coefficient, $\dot{\Omega}/\Omega = \dot{\varepsilon}_V$ the skeleton volumetric deformation rate and k_s is the grain compressibility. The porosity variation is used in the fluid balance equations (eq. (3) and (4)) in the computation of the storage term. It introduces a coupling term between the mechanical behaviour and the fluid transfers.

2.2.3. Fluid transport constitutive equations

A biphasic flow model is considered for the description of the fluid transport processes. The liquid phase may contain dissolved air and the gas phase is a mixture of dry air and water vapour. The fluid fluxes are described by the advection of each phase and by the diffusion of the species in each phase. The following relationships are written for the particular case of a binary fluid mixture composed by water and air, but can be easily extended for other binary fluid mixtures of water and other gas species (hydrogen, nitrogen, helium, argon…). More details are available on section 2.5.

2.2.3.1. Advective flux of the liquid phase

The advective flux of the liquid phase is governed by the Darcy's law:

$$\underline{q}_l = -\frac{\underline{\underline{K}}_w \, k_{rw}}{\mu_w}\left(\underline{grad}\left(p_w\right) + \rho_w g.\underline{grad}\left(y\right)\right) \tag{9}$$

where $\underline{\underline{K}}_w$ is the water intrinsic permeability tensor, k_{rw} is the water relative permeability, μ_w is the water dynamic viscosity, g the gravity acceleration and y the vertical upward directed coordinate.

2.2.3.2. Advective flux of the gaseous phase

The advective flux of the gaseous phase is governed by the Darcy's law:

$$\underline{q}_g = -\frac{\underline{\underline{K}}_g \, k_{rg}}{\mu_g}\left(\underline{grad}\left(p_g\right) + \rho_g g.\underline{grad}\left(y\right)\right) \tag{10}$$

where $\underline{\underline{K}}_g$ is the gas intrinsic permeability tensor, k_{rg} is the gas relative permeability, μ_g is the dynamic viscosity of the gaseous mixture, g the gravity acceleration and y the vertical upward directed coordinate.

The dynamic viscosity of the gaseous mixture depends on the dynamic viscosity of each component of the mixture:

$$\mu_g = \frac{1}{\dfrac{\rho_a}{\rho_g \mu_a} + \dfrac{\rho_v}{\rho_g \mu_v}} \tag{11}$$

with ρ_a and ρ_v the density respectively of the dry air and the water vapour, and μ_a and μ_v the dynamic viscosity respectively of the dry air and the water vapour.

Other relationships exist for the dynamic viscosity of a gaseous mixture. For instance, in the Lagamine code, the dynamic viscosity of the dry air – water vapour mixture is expressed by (Wilke, 1949):

$$\mu_g = \frac{\mu_a}{1 + \dfrac{\left(X_v/X_a\right)\left(1+\sqrt{\mu_a/\mu_v}\sqrt[4]{M_v/M_a}\right)^2}{2\sqrt{2}\sqrt{1+\left(M_a/M_v\right)}}} + \frac{\mu_v}{1 + \dfrac{\left(X_a/X_v\right)\left(1+\sqrt{\mu_v/\mu_a}\sqrt[4]{M_a/M_v}\right)^2}{2\sqrt{2}\sqrt{1+\left(M_v/M_a\right)}}} \tag{12}$$

with $X_a = p_a / p_g$ the air molar fraction and $X_v = p_v / p_g$ the vapour molar fraction.

2.2.3.3. Non-advective flux of water vapour and dry air

The non-advective flux of water vapour, i.e. diffusive flux, is related to the water vapour bulk density gradient (Fick's law):

$$\underline{i}_v = -\phi\left(1-S_{r,w}\right)\tau D_{v/a}\rho_g \underline{grad}\left(\frac{\rho_v}{\rho_g}\right) = -\underline{i}_a \tag{13}$$

where $D_{v/a}$ is the diffusion coefficient in the gaseous mixture dry air – water vapour and τ is the tortuosity of the porous medium.

The diffusion coefficient depends on temperature and gas pressure. Two relations are commonly used: the first one for gaseous mixture of dry air and water vapour (Philip and de Vries, 1957), the second one for gaseous mixture of another gas species *i* and water vapour:

$$D_{v/a} = 5,893.10^{-6}\frac{T^{2,3}}{p_g} \tag{14}$$

$$D_{v/i} = D_0\left(\frac{p_{g0}}{p_g}\right)\left(\frac{T}{T_0}\right)^{1,75} \tag{15}$$

where D_0 is the diffusion coefficient for a given gas mixture.

2.2.3.4. Non-advective flux of dissolved air

The non-advective flux of dissolved air in the liquid phase, i.e. diffusive flux, is related to the dissolved air bulk density gradient (Fick's law):

$$\underline{i}_{a-d} = -\phi S_{r,w}\tau D_{a-d/w}\rho_w \underline{grad}\left(\frac{\rho_{a-d}}{\rho_w}\right) \tag{16}$$

where ρ_{a-d} is the density of the dissolved air and $D_{a-d/w}$ is the diffusion coefficient of dissolved air in water, which depends on temperature.

2.2.4. Liquid density variation

The compressible fluid is assumed to respect the following relationship (Lewis and Schrefler, 2000). This predicts an increase of water density as a function of the water pressure, defining χ_w as the liquid water bulk modulus:

$$\dot{\rho}_w = \frac{\rho_w}{\chi_w}\dot{p}_w \tag{17}$$

2.2.5. Gas density variation

For a gaseous mixture of dry air and water vapour, the ideal gas law is introduced, because the moist air is assumed to be a perfect mixture of two ideal gases. The equation of state of perfect gas (Clapeyron's equation) and Dalton's law applied to dry air, water vapour and moist air yields (Pollock, 1986; Gawin et al., 1996):

$$p_a = \frac{\rho_a RT}{M_a} \text{ and } p_v = \frac{\rho_v RT}{M_v} \tag{18}$$

$$p_g = p_a + p_v \text{ and } \rho_g = \rho_a + \rho_v \tag{19}$$

with M_a and M_v the molar mass respectively of the dry air and the water vapour.

2.2.6. Water absorption / desorption

The relation between the amount of water present in soil pore space (quantified by the degree of saturation of liquid $S_{r,w}$ or the water content w) and the soil suction s is usually referred to as the water retention curve. Different analytical expressions of the water retention curve have been proposed, based on various meaningful soil characteristics to provide a continuous relation between soil suction and the degree of saturation.

2.2.6.1. Reversible retention curve

The van Genuchten relationship reads:

$$S_{r,we} = \frac{S_{r,w} - S_{res}}{S_{\max} - S_{res}} = \left(1 + \left(\frac{s}{\mathrm{P}_r}\right)^{\frac{1}{1-m}}\right)^m \tag{20}$$

where $S_{r,we}$ is effective saturation of porous media, S_{res} is the residual degree of saturation, $S_{\max}$ is the maximum degree of saturation, s is the suction, P_r is the pressure of air entrance, m is the shape function coefficient.

Other classical retention curves are proposed or could be defined by user in the different finite element codes, as the Vauclin relationship:

$$S_{r,we} = \frac{S_{r,w} - S_{res}}{S_{\max} - S_{res}} = \frac{a}{a + (b.s)^{\lambda}} \tag{21}$$

with a, b and λ the material parameters.

2.2.6.2. Retention curve with hysteresis behaviour - Lagamine

Experimental data show that the process of desaturation occurs only at suction values greater than the air entry-suction. Below this limit, the soil remains saturated while suction is positive. Experimental data show also a hysteretic behaviour of the retention behaviour. At the same suction, the degree of saturation is lower on a wetting path (water absorption) than on a drying path (water desorption). A water retention constitutive model, considering the effects of hysteresis and air entry-suction and proposed by François (2008), is introduced in the Lagamine code. Hysteresis in water retention behaviour is modelled as a plastic process, assuming an analogy between the air-entry suction s_e (yield limit in the ($S_{r,w} - s$ plane) and the preconsolidation pressure p_c' (yield limit in the isotropic mechanical plane). Under re-wetting, a hysteretic phenomenon occurs, also represented by a yielding process. Two plastics mechanisms are considered, respectively for drying and wetting paths:

$$f_{dry} \equiv s - s_d = 0 \tag{22}$$

$$f_{wet} \equiv s_d s_{hys} - s = 0 \tag{23}$$

where s_d is the drying yield limit and s_{hys} a material parameter considering the size of the water retention hysteris. If the initial state is saturated, the initial drying limit s_{d0} is equal to air-entry suction s_e and increases when suction overtakes s_e as follows:

$$s_d = s_{d0} \exp\left(-\beta_h \Delta S_{r,w}\right) \tag{24}$$

where β_h is the slope of the desaturation curve in the $\left(S_{rw} - \ln s\right)$ plane.

2.2.7. Permeability variation

The permeability tensor $\underline{\underline{K}}_p k_{rp}$ $\left(p = w, g\right)$ can depend on the degree of saturation for unsaturated cases or on the mechanical behaviour (porosity or tensile strain). Different constitutive models exist to reproduce the permeability tensor evolution.

2.2.7.1. Water permeability variation with degree of saturation

The advective fluxes of the liquid and gaseous phases are governed by the Darcy's law for unsaturated cases. In this relation, it is assumed that the effective permeability tensor depends on the degree of saturation. A water relative permeability function k_{rw} is introduced, reproducing the decrease of the water permeability with the drying of the material. Different models exist and are introduced in the finite element codes.

The van Genuchten function reads:

$$k_{rw} = \sqrt{S_{r,w}} \left(1 - \left(1 - S_{r,w}^{\frac{1}{m}} \right)^{m} \right)^{2} \tag{25}$$

with *m* a material parameter coming from the van Genuchten's water retention curve (equation 20).

Water relative permeability can be also expressed as a power of degree of saturation. Cubic law is generally used:

$$k_{rw} = \left(S_{r,w} \right)^{3} \tag{26}$$

Other functions could be defined easily by user.

2.2.7.2. Gas permeability variation with degree of saturation

As for the water relative permeability, a gas relative permeability can be introduced in the Darcy's law for unsaturated cases in order to reproduce the increase of the permeability tensor with the degree of saturation. An extension of the van Genuchten – Mualem can be used:

$$k_{rg} = \sqrt{1 - S_{r,w}} \left(1 - S_{r,w}^{\frac{1}{m}} \right)^{2m} \tag{27}$$

with *m* a parameter coming from the van Genuchten's water retention curve .

Gas relative permeability can be also expressed as a power of degree of saturation. Cubic law is generally used:

$$k_{rg} = \left(1 - S_{r,w} \right)^{3} \tag{28}$$

Other functions could be defined easily by user.

2.2.7.3. Permeability variation with porosity

The influence of the mechanical behaviour of the material on the permeability tensor can be modelled by different ways. The permeability tensor $\underline{\underline{K}}$ can depend on porosity through Kozeny-Karman's law:

$$\underline{\underline{K}} = \underline{\underline{K}}_{0} \left(\frac{\phi}{\phi_0} \right)^{3} \left(\frac{1 - \phi_0}{1 - \phi} \right)^{2} \tag{29}$$

where $\underline{\underline{K}}_{0}$ is the initial permeability, ϕ is the porosity, ϕ_0 is the initial porosity.

Other relationships take into account the coupling between permeability and porosity, as the one used in GDR Momas and developed in the Lagamine code or in Code_Aster:

$$\underline{\underline{K}} = \underline{\underline{K}}_0 \left(1+\alpha\left(\phi-\phi_0\right)^{\beta}\right) \tag{30}$$

where α and β are material parameters.

2.2.7.4. Embedded fracture model – Code Bright & Lagamine

A specific permeability model (Olivella and Alonso, 2008; Arnedo et al., 2008; Alonso et al., 2006; Levasseur et al., 2010) can be considered for the argillaceous rocks in WP4. The embedded fracture model is available in Code_Bright and Lagamine. The basic idea consists in the appropriate representation of single discontinuity representing the rock bedding, which is embedded in a continuous finite element. Figure 1 shows, in the left part, a single fracture in a porous medium characterized by its aperture *b* and, on the right, a finite element composed by a rock matrix (in general, a porous medium) and a series of *n* fractures. The number of fractures in an element depends on the width associated with each fracture, *a*, which will be considered a characteristic size of the material, and the element size *s* (perpendicular to the direction of discontinuities).

Liquid and gas flow through a single planar fracture is calculated using Darcy's law. The intrinsic permeability can be calculated, assuming laminar flow, as:

$$K_{fracture} = \frac{b^2}{12} \tag{31}$$

where *b* is the aperture of the single fracture.

When a set of *n* fractures is included in a finite element (Figure 1), the equivalent intrinsic permeability K_{ij} of the element in the direction parallel to the fractures can be calculated as:

$$K_{ij} = K_{matrix}\left(\frac{s-nb}{s}\right)+\sum_{i=1}^{n}\left(K_{fracture}\frac{b}{a}\frac{a}{s}\right) = K_{matrix}\left(\frac{s-nb}{s}\right)+\sum_{i=1}^{n}\left(K_{fracture}\frac{b}{a}\frac{1}{n}\right) \cong K_{matrix}+\frac{b^3}{12a} \tag{32}$$

where K_{matrix} is the reference intrinsic permeability of the rock matrix or porous material, i.e. the material without fractures, *s* is the element size (width normal to flow direction), *a* is the width associated with each fracture, and $n = s / a$ is the number of fractures in the element. Permeability of the matrix will be relevant only for very low apertures; otherwise fracture permeability will dominate the total permeability and matrix permeability will be negligible in comparative terms.

The aperture of the fracture can be estimated as a function of deformation in the following way:

$$\begin{aligned} &b = b_o + \Delta b \quad \text{for} \quad \Delta b \geq 0 \\ &\Delta b = a\Delta\varepsilon = a(\varepsilon-\varepsilon_o) = (s/n)(\varepsilon-\varepsilon_o) \quad \text{for} \quad \varepsilon > \varepsilon_o \end{aligned} \tag{33}$$

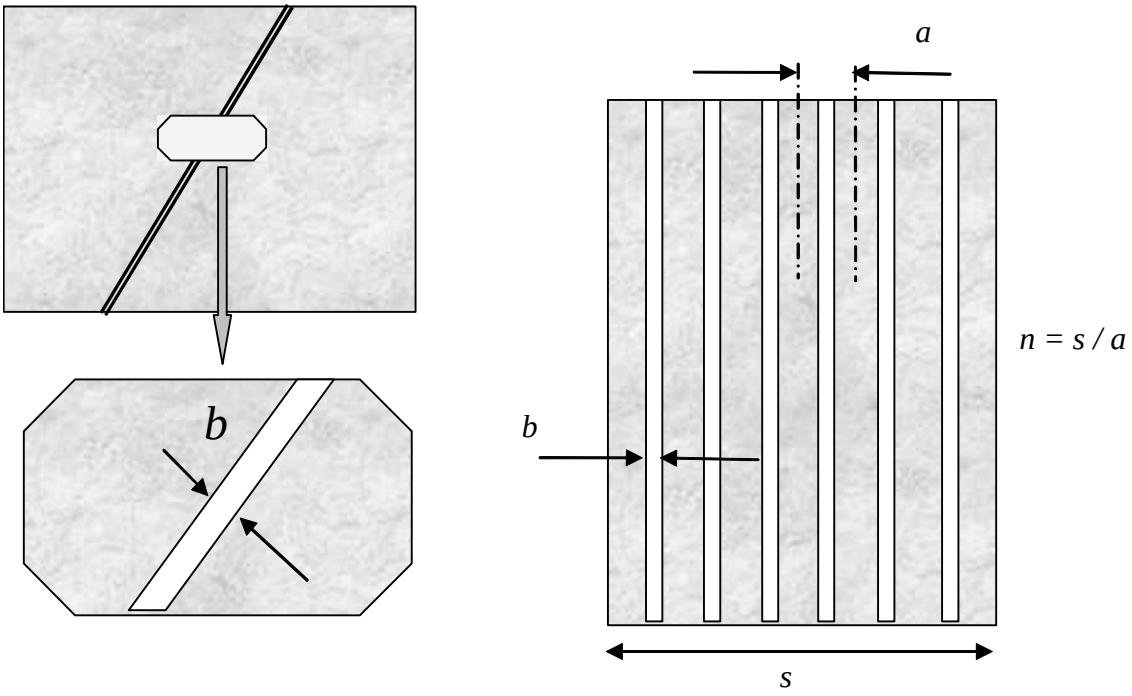

Figure 1. A single fracture characterized by its aperture *b* (left) and a finite element with a series of parallel fractures (right). The width of the element is *s*, the aperture of the fractures is *b*, the associated width to each fracture is *a*, and the number of fractures in the element is *n*.

It has been assumed that deformation is localized and results in changes in aperture. A threshold value (ε_o) is considered. Therefore the changes in aperture start when deformation reaches this value. Deformation perpendicular to the fracture plane is to be used when aperture changes have to be obtained. The threshold value (ε_o) is associated with fracture initiation. This parameter will be set to zero if the fractures already exist and have an initial aperture b_o. The initial aperture can be also zero when the fractures exist but are closed.

The variation of capillary pressure induced by fracture aperture changes is also included in the Code_Bright (but not in Lagamine code). According to Kelvin's law the capillary pressure necessary to desaturate a fracture is given by:

$$P_o = \sigma\left(\frac{1}{r_1}+\frac{1}{r_2}\right)=\frac{2\sigma}{b} \tag{34}$$

with σ the surface tension. It is obtained when $(1/r_1) = 0$ and $r_2 = b/2$ (the wetting angle has been assumed to be 0). This equation can be used directly to calculate the air entry value of the element. If equation (30) is combined with equation (28) the capillary pressure to start desaturation is obtained as:

$$P_r = P_o \frac{\sqrt[3]{K_{ij,o}}}{\sqrt[3]{K_{ij}}} \tag{35}$$

where P_0 is the capillary pressure for a reference permeability K_o, which eventually can be the initial permeability. As a first approximation the capillary pressure associated with the

discontinuity can be introduced in the standard water retention curve of van Genuchten (van Genuchten, 1980).

2.3. Equilibrium restrictions

2.3.1. Kelvin's law

It is assumed that the water vapour in porous media is always in equilibrium with the liquid water. The corresponding equilibrium restriction equation is given by Kelvin's law for the vapour concentration in the gaseous phase:

$$RH = h_r = \frac{p_v}{p_{v0}} = \exp\left(\frac{-sM_v}{RT\rho_w}\right) \tag{36}$$

where $RH = h_r$ is the relative humidity, p_v is the partial vapour pressure, p_{v0} is the water vapour saturation pressure at the same temperature, s is the suction, M_v is the molecular mass of water vapour (0.018 kg/mol), R is the universal gas constant (8.314 J/(mol K)) and T is the absolute temperature in Kelvin.

The water vapour saturation pressure p_{v0} is the vapour pressure in equilibrium with liquid water pressure if the capillary effects are not considered. The saturated vapour concentration can be obtained by two empirical relationships. The first one is based on experimental date from Ewen et al. (1989) and is used in the Lagamine code or in Code_Aster:

$$\frac{1}{\rho_{v0}} = 194,4\exp\left(-0,06374\left(T-273\right)+0,1634.10^{-3}\left(T-273\right)^2\right) \tag{37}$$

for temperature range between 293 K and 331 K.

Other relation gives an adequate estimation, based on data from Garrels & Christ (1965):

$$p_{v,0}\left(MPa\right) = 112659.\exp\left(\frac{-5192,74}{T}\right) \tag{38}$$

for temperature range between 273 K and 373 K.

2.3.2. Henry's law

The amount of dissolved air in the liquid phase is always in equilibrium and proportional with the quantity of dry air. The amount of dissolved air is given by Henry's law (Weast, 1971).

$$\rho_{a-d} = H_a\left(T\right)\rho_a \tag{39}$$

where H_a is Henry's coefficient for dissolved air, depending on temperature.

2.4. Water parameters for fluid transport relations

The constitutive equations proposed for a binary mixture of water and air depends on some parameters of water (liquid water or water vapour), defined in the
Table **1**.

		Liquid water	**Water vapour**	
Dynamic viscosity	μ	10^{-3}	10^{-5}	Pa.s
Density	ρ	1000	Psychrometric restriction	kg/m³
Bulk modulus	χ	$2\ 10^{9}$	Ideal gas relation	Pa

Table 1 : Main water parameters for fluid transport relations for T=20°C and p_w=p_g=0.1 MPa

2.5. Gas parameters for fluid transport relations

The general framework for the modelling of unsaturated porous media previously described assumes a binary fluid mixture: water and air. The balance equations and the constitutive relations can be extended when other binary fluid mixtures are considered, especially for water and other gas species (hydrogen, nitrogen, helium, argon…). In these cases, the presence of air in the porous media is neglected. Even tough the constitutive equations are similar, parameters of the models depend on the gas species, as presented in the Table 2.

		Air	**Hydrogen**	**Nitrogen**	**Helium**	**Argon**	
Dynamic viscosity	μ_a	$18{,}6\ 10^{-6}$	$9\ 10^{-6}$	$17{,}9\ 10^{-6}$	$20\ 10^{-6}$	$22{,}9\ 10^{-6}$	Pa.s
Diffusion coefficient in gaseous phase with water vapour	D_0	Equation (14)	$9{,}5\ 10^{-5}$	$2{,}42\ 10^{-5}$	$7{,}81\ 10^{-5}$	$3{,}04\ 10^{-5}$	m²/s
Diffusion coefficient of dissolved gas in liquid phase	$D_{a-d/w}$	$5{,}03\ 10^{-9}$	$4{,}6\ 10^{-9}$	$2\ 10^{-9}$	$7{,}28\ 10^{-9}$	$2{,}5\ 10^{-9}$	m²/s
Density	ρ_a	1,205	0,0838	1,1652	0,1663	1,6619	kg/m³
Henry's coefficient	H_a	0,0234	0,0190	0,0149	0,0091	0,0342	-

Table 2 : Main gas parameters for fluid transport relations for T=20°C and p_w=p_g=0.1 MPa

3. Conclusions

In the framework of the European Forge project, modelling of laboratory or in-situ gas migration tests will be performed by Université de Liège, Electricité de France and Universitat Politècnica de Catalunya. The different finite element codes are Lagamine (ULg), Aster (EDF) and Code_Bright (UPC). All these codes deal with thermo-hydro-mechanical problems with partial saturation in porous media, including the gas transfers.

In this report, the initial state of the numerical codes and the main conceptual models existing at the beginning of the project have been described. The general framework for unsaturated porous media has been presented. The constitutive equations of the mechanical and the fluid transfers problems have been described. The main differences between the finite element codes have been highlighted. It mainly concerns the description of the permeability tensor evolution with the mechanical behaviour. Finally, a review of the values of the main water and gas fluid parameters has been presented.

4. References

Arnedo D., Alonso E.E., Olivella S., Romero E. 2008. Gas injection tests on sand/bentonite mixtures in the laboratory. Experimental results and numerical modelling. *Physics and Chemistry of the Earth*. **33** Suplement, 237- 247, doi:10.1016/j.pce.20.

Alonso E.E., Gens A., Josa A. 1990. A constitutive model for partially saturated soils. *Géotechnique*. **40**(3), 405-430.

Alonso E.E., Olivella S., Arnedo D. 2007. Mechanisms of gas transport in clay barriers. *Journal of Iberian Geology*. **32(**2), 175–196.

Biot M.A. 1941. General theory of three-dimensional consolidation. *Journal of Applied Physics*. **12**, 155-164.

Carol I., Rizzi E., Willam K. 2001. On the formulation of anisotropic elastic degradation. Theory based on a pseudo-logarithmic damage tensor rate. *International Journal of Solids and Structures*. **38**(4), 491-518.

Coussy O. 1995. *Mechanics of Porous Continua*. Wiley, London.

Coussy O. 2004. *Poromechanics*. Wiley, London.

Ewen J., Thomas H.R. 1989. Heating unsaturated medium sand. *Géotechnique*. **3**, 455-470.

François B. 2008. *Thermo-Plasticity of Fine-Grained Soils at Various Saturation States: Application to Nuclear Waste Disposal*. PhD. Thesis. Ecole Polytechnique Fédérale de Lausanne, 334 p.

Garrels R.M., Christ C.L. 1965. *Solutions, Minerals, and Equilibria.* New-York: Harper & Row, 450 p.

Gawin D., Schrefler B.A. 1996. Thermo-hydro-mechanical analysis of partially saturated porous materials. *Engineering Computations*. **13(**7), 113-143.

Hassanizadeh M., Gray W. 1979. General conservation equations for multi-phase systems: 1. Average procedure. *Advances in Water Resources*. **2**, 131–144.

Hassanizadeh M., Gray W. 1979. General conservation equations for multi-phase systems: 2. Mass, momenta, energy, and entropy equations. *Advances in Water Resources*. **2**, 191–208.

Levasseur S., Charlier F., Frieg B., Collin F. 2010. Hydro-mechanical modelling of the excavation damaged zone around an underground excavation at Mont Terri Rock Laboratory. *International Journal of Rock Mechanics & Mining Sciences*, doi:10.1016/j.ijrmms.2010.01.006.

Lewis RW., Schrefler B.A. 2000. *The Finite Element Method in the Static and Dynamic Deformation and Consolidation of Porous Media*. Wiley, New York.

Nuth M., Laloui L. 2008. Effective stress concept in unsaturated soils: Clarification and validation of a unified framework. *International Journal for Numerical and Analytical Method in Geomechanics*. **32**, 771–801.

Olivella S., Gens A., Carrera J., Alonso E.E. 1996. Numerical formulation for a simulator (CODE_BRIGHT) for the coupled analysis of saline media. *Engineering Computations*. **13**(7), 87-112.

Olivella S., Carrera J., Gens A., Alonso E.E. 1994. Nonisothermal multiphase flow of brine and gas through saline media. *Transport in Porous Media*. **15**, 271-293.

Olivella S., Alonso E.E. 2008. Gas flow through clay barriers. *Géotechnique*. **58**(3), 157–176.

Panday S., Corapcioglu M.Y. 1957. Reservoir transport equations by compositional approach. *Transport in Porous Media*. **4,** 369-393.

Philip J.R., de Vries D.A. 1957. Moisture movement in porous materials under temperature gradients. *EOS Trans. AGU.* **38**(2), 222–232.

Pollock D.W. 1986. Simulation of Fluid Flow and Energy Transport Processes Associated With High-Level Radioactive Waste Disposal in Unsaturated Alluvium. W*ater Resources Research*. **22**(5), 765-775.

van Genuchten M. Th. 1980. Closed-form equation for predicting the hydraulic conductivity of unsaturated soils. *Soil Sci. Soc. Am. J*. **44**, 892-898.

Weast R.C. 1971. *Handbook of Chemistry and Physics*. **51** (Ed. CRC Press), Cleveland.

Wilke C.R. 1950. A Viscosity Equation for Gas Mixtures. *Journal of Chemical Physics*. **18**(4), 517-519.

Wittke W. 1990. *Rock mechanics: theory and applications with case histories.* Springer-Verlag.

5. Appendix

5.1. Damage – Elastoplastic model – Mathematical formulation - UPC

The mathematical formulation of the damage – elastoplastic model proposed by UPC is described hereafter. For this model, equations are written assuming soils mechanics compression ($p > 0$, $\varepsilon_v > 0$ for compression). p is the mean effective stress, J the square root of the second invariant of deviatoric stress tensor, θ the Lode' angle (-30º in triaxial compression, +30º in triaxial extension).

Clay matrix behaviour

Elastic law:

$$d\sigma_{ij}^{M} = D_{ijkl}^{eM}\left(d\varepsilon_{ij}^{M} - d\varepsilon_{kl}^{p}\right) \tag{40}$$

D_{ijkl}^{eM} is defined by a transversal isotropic elastic model based on the model presented by Wittke (1990), which considers 5 material parameters plus 2 anisotropy directions describing the bedding orientation.

Yield function: 2 kind of yield criteria are considered

Mohr-Coulomb:

$$F^{p} = \left(\cos\theta^{M} + \frac{1}{\sqrt{3}}\sin\theta^{M}\sin\phi'\right)J^{M} - \sin\phi'(p^{M} + p_{t}) \geq 0 \tag{41}$$

$p_t = c'\cot\phi'$ is clay matrix tensile strength, *c'* clay matrix cohesion, ϕ' clay matrix friction angle.

Hoek & Brown (1980):

$$F^{p} = \frac{4\sin^{2}\left(\theta^{M} - \frac{\pi}{6}\right)}{R_{c}}J^{M2} - \frac{2\ m\sin\theta^{M}}{\sqrt{3}}\ J^{M} - m(p^{M} + p_{t}) \geq 0 \tag{42}$$

$p_t = R_c / m$ is clay matrix tensile strength, R_c clay matrix uniaxial compressive strength, *m* a parameter defining the shape of the parabolic yield criterion.

Both yield criteria present corners in the deviatoric plane. They are smoothed using Sloan & Booker (1986) procedure. Lode's angle θ_t at which smoothing starts must be defined (see ICL = 74).

Rate dependency: Rate dependency is introduced as a visco-plastic mechanism. Plastic multiplier λ^p is expressed as a function of the distance between the current clay matrix stress point and the inviscid plastic locus:

$$d\lambda^{p} = \frac{dt}{\eta_{M}}\left\langle F^{p}\right\rangle \tag{43}$$

where *dt* is the time increment, η_M is the clay matrix viscosity and $\langle\rangle$ are the Macauley brackets. Inviscid plastic locus takes the form:

$$\bar{F}^{p} = F^{p} - \frac{\eta_{M}}{dt}d\lambda^{p} \leq 0 \tag{44}$$

where F^p can be either the Mohr Coulomb or Hoek & Brown yield criterion.

Plastic potential: a non associated plastic potential in the p-q diagram is defined for each yield criterion. In the deviatoric plane, plastic potential is considered associated.

Mohr-Coulomb:

$$F^p = \left(\cos\theta^M + \frac{1}{\sqrt{3}} \sin\theta^M \sin\phi' \right) J^M - \omega \sin\phi' (p^M + p_t) \geq 0 \qquad (45)$$

p_t, c' and ϕ' are parameters defining the yield criterion. ω is a parameter defining the non associativity of the flow. It takes a value equal to 1 when associated and equal to 0 for null dilatancy.

Hoek & Brown:

$$F^p = \frac{4\sin^2\left(\theta^M - \frac{\pi}{6}\right)}{R_c} J^{M2} - \frac{2 \ m\sin\theta^M}{\sqrt{3}} \ J^M - \omega m (p^M + p_t) \geq 0 \qquad (46)$$

p_t, R_c and m are parameters defining the yield criterion. ω is a parameter defining the non associativity of the flow. It takes a value equal to 1 when associated and equal to 0 for null dilatancy.

Hardening law: in the case in which only matrix behaviour is considered (bonds constitutive law is not activated), it is possible to define a degradation law for the plastic hardening parameter. If bonds are considered, degradation is due to bond degradation and matrix behaviour is considered perfectly plastic.

Mohr-Coulomb:

$$p_t = c'_0 \operatorname{cotan}\phi' \left[1 - (1-\alpha) \frac{\max(\varepsilon_1^p, \xi_r)}{\xi_r} \right] \qquad (47)$$

c'_0 is the intact cohesion, α a brittleness parameter, ε^p_1 is the major principal plastic strain, ξ_r the accumulated major principal plastic strain at which the residual cohesion $\alpha c'_0$ is reached. $\alpha = 1$ means perfect plasticity, $\alpha = 0$, total degradation (residual cohesion equal to 0).

Hoek & Brown:

$$p_t = \frac{R_{c0}}{m} \left[1\text{-}(1-\alpha) \frac{\max(\varepsilon_1^p, \xi_r)}{\xi_r} \right]^2 \qquad (48)$$

R_{c0} is the intact strength, α a brittleness parameter, ε^p_1 is the major principal plastic strain, ξ_r the accumulated major principal plastic strain at which the residual strength $\alpha^2 R_{c0}$ is reached. $\alpha = 1$ means perfect plasticity, $\alpha = 0$, total degradation (residual strength equal to 0).

Bond behaviour

Elastic law:

$$d\sigma_{ij}^{b} = D_{ijkl}^{eb}\left(d\varepsilon_{ij}^{b} - d\varepsilon_{kl}^{d}\right) \tag{49}$$

D_{ijkl}^{eb} is the secant damaged elastic matrix. It is related to the secant undamaged elastic tensor D_{ijkl}^{eb0} by $D_{ijkl}^{eb} = e^{-L} D_{ijkl}^{eb0}$. L is the damage variable, related to the ratio of bond mickocraks area over the whole bond area. D_{ijkl}^{eb0} is defined by the undamaged bond Young's modulus E_b and bond Poisson's ratio ν_b through the classical linear isotropic elasticity.

Damage locus: Damage locus is defined as an energy threshold

$$F^{d} = \frac{1}{2}\sigma_{ij}^{b}\varepsilon_{ij}^{b} - r^{b} \tag{50}$$

r_b is the value of energy threshold.

Rate dependency: Rate dependency is introduced as a delayed microcracking and use the visco-damage formalism. Damage variable is expressed as a function of the distance between the current bond stress point and the infinitely slow damage locus:

$$dL = \frac{dt}{\eta_b}\left\langle F^{d}\right\rangle \tag{51}$$

where dt is the time increment, η_b is the bond viscosity and $\langle\rangle$ are the Macauley brackets. Infinitly low damage locus takes the form:

$$\bar{F}^{d} = F^{d} - \frac{\eta_b}{dt}dL \le 0 \tag{52}$$

Damage rule: Damage rule gives the evolution of damage strain $d\varepsilon_{kl}^{d}$ with damage variable L. This relation is constrained by bond elastic moduli evolution and must take the form:

$$d\varepsilon_{kl}^{d} = \varepsilon_{ij}^{b} dL \tag{53}$$

Damage evolution law: It gives the evolution of damage locus r_b with damage variable L. A simple linear expression is considered:

$$r^{b} = r_0 + r_1 L \tag{54}$$

r_0 is the damage of the intact material and r_1 a parameter giving the rate of evolution (higher value of r_1 gives lower damage rate).

Coupling behaviour: Coupling comes from the restrictions that local strain ε_{ij}^{M} and ε_{ij}^{b} must be compatible with the external strain ε_{ij} and local stresses σ_{ij}^{M} and σ_{ij}^{b} must be in equilibrium with external stresses σ_{ij} . These restrictions read:

$$d\varepsilon_{ijM} = d\varepsilon_{ij} + d\varepsilon_{ijb} \tag{55}$$

$$\sigma_{ij} = (1+\chi)\sigma_{ijM} + \chi\sigma_{ijb} \text{ with } \chi = \chi_0 e^{-L/2} \tag{56}$$

L is the damage variable and χ_0 a coupling parameter that gives the relative importance of bond and clay matrix behaviour in the overall response of the composite material.

5.2. Drücker-Prager Viscoplastic model – Mathematical formulation - EDF

This section will describe the mathematical formulation of the viscoplastic model based on Drücker Prager criterion developped in Code_Aster. The proposed model is based on only one viscoplastic mechanism. The viscoplastic criterion hardening is due to the cumulated deviatoric plastic deformation, passing through three steps called thresholds: the initial threshold for a null viscoplastic deformation, the peak threshold for a peak deformation (parameter of the model) and a final threshold for a deformation beyond the ultim one (a parameter of the model). The stress state can be out of the threshold but it turns back with a speed proportional to the distance between the stress state and the threshold according to Perzyna law. The flow is not associated, the flow potential is a Drucker-Prager one which hardens according to three levels (initial, peak, and ultim). Between the thresholds, hardening is linear.
In the following, p is the accumulated viscoplastic strain, S_{II} the second invariant of deviatoric stress tensor, I_1 the first invariant of stress, D_e the elastic tensor.

In this model, the yield surface is defined by :

$$f = \sqrt{\frac{3}{2}} S_{II} + \alpha(p) I_1 - R(p)$$

with, $\alpha(p)$, $R(p)$ function of p.
The viscoplastic potential G is defined by

$$G = \sqrt{\frac{3}{2}} S_{II} + \beta(p) I_1$$

To describe evolution of f and G, three levels are defined corresponding to three thresholds ; the initial one matches the elastic part without viscoplastic deformation, the peak threshold the peak threshold which caracterizes the maximal stress state and a final threshold corresponding to the residual state. Between the initial and the peak thresholds the behaviour is hardening. Between the peak and the residual thresholds the behaviour is softening.

We note thereafter :
α_0, R_0, β_0 hardening parameters linked to elastic threshold $(p = 0)$
$\alpha_{pk}, R_{pk}, \beta_{pk}$ hardening parameters linked to peak threshold $(p = p_{pk})$
$\alpha_{ult}, R_{ult}, \beta_{ult}$ hardening parameters linked to final threshold $(p = p_{ult})$

Then, Cohesion functions are defined as following:

$$\begin{cases} \alpha(p) = \left(\dfrac{\alpha_{pk} - \alpha_0}{p_{pk}} \right) p + \alpha_0 \ \ pour\ 0 < p < p_{pk} \\ \alpha(p) = \left(\dfrac{\alpha_{ult} - \alpha_{pk}}{p_{ult} - p_{pk}} \right) \left(p - p_{pk} \right) + \alpha_{pk} \ \ pour\ \ p_{pk} < p < p_{ult} \\ \alpha(p) = \alpha_{ult} \ \ pour\ \ p > p_{ult} \end{cases}$$

the dilatancy functions are:

$$\begin{cases} \beta(p) = \left(\dfrac{\beta_{pk} - \beta_0}{p_{pk}} \right) p + \beta_0 \ \ pour\ 0 < p < p_{pk} \\ \beta(p) = \left(\dfrac{\beta_{ult} - \beta_{pk}}{p_{ult} - p_{pk}} \right) \left(p - p_{pk} \right) + \beta_{pk} \ \ pour\ \ p_{pk} < p < p_{ult} \\ \beta(p) = \beta_{ult} \ \ pour\ \ p > p_{ult} \end{cases}$$

and the hardening functions:

$$\begin{cases} R(p) = \left(\dfrac{R_{pk} - R_0}{p_{pk}} \right) p + R_0 \ \ pour\ 0 < p < p_{pk} \\ R(p) = \left(\dfrac{R_{ult} - R_{pk}}{p_{ult} - p_{pk}} \right) \left(p - p_{pk} \right) + R_{pk} \ \ pour\ \ p_{pk} < p < p_{ult} \\ R(p) = R_{ult} \ \ pour\ \ p > p_{ult} \end{cases}$$

Stress and strains are linked with a classical hooke's law:

$\sigma = D_e \left(\varepsilon - \varepsilon^{vp} \right)$

The viscoplastic deformation is controled by the Perzyna law:

$$d\varepsilon_{ij}^{vp} = A \left\langle \frac{f}{p_{ref}} \right\rangle^n \frac{\partial G}{\partial \sigma_{ij}} dt$$

with p_{ref} the reference pressure (atmospheric pressure) and A creeping parameter.